Electrochemical discharge machining of a high-precision micro-holes array in glass wafer using a damping and confinement technique

Zhixiang Zou [a, b], Kangcheung Chan [b, *], Shunzhi Qiao [a], Kai Zhang [a], Taiman Yue [b], Zhongning Guo [a], Jiangwen Liu [a, *]

[a] State Key Laboratory of Precision Electronic Manufacturing Technology and Equipment, Guangdong University of Technology, Guangzhou 510006, PR China

[b] Research Institute for Advanced Manufacturing, Department of Industrial and Systems Engineering, The Hong Kong Polytechnic University, Hung Hom, Hong Kong

*Corresponding author: Kangcheung Chan.

Email: kc.chan@polyu.edu.hk

*Corresponding author: Jiangwen Liu.

Email: fejwliu@scut.edu.cn

ABSTRACT

Due to the unstable gas film, it is still a big challenge to achieve high repeatability and quality in electrochemical discharge machining (ECDM) of micro-hole array in glass. Based on our previous research on ECDM of micro channels, the present work uses a non-Newtonian fluid electrolyte (non-NTF electrolyte) in ECDM to further achieve a high uniformity-precision and quality micro-holes array in glass through the damping and confinement effect. The results revealed that an average entrance diameter of 343.8 ± 3.47 μm (mean ± standard deviation) and average heat-affected zone (HAZ) width

of 18.01 ± 1.52 μm were successfully fabricated in the 300-μm-thick glass wafer. As compared to the conventional KOH electrolyte, the entrance overcut and the HAZ width of micro-holes were reduced by 43.84%, and 64.81%, respectively, while the repeatability improved by 67.92%. The non-NTF electrolyte concentration and the tool rotation speed was also found to play a significant role in the damping and confinement effect, significantly affecting the geometrical properties of micro-holes. Furthermore, the micro-holes array was filled with copper to form a through glass vias (TGVs), and a standard deviation of the Kelvin resistance of TGVs was only 5.35 mΩ, further demonstrating an excellent repeatability and localization of ECDM micro-holes using a non-NTF electrolyte. The results illustrate that employing a non-NTF electrolyte is a simple way to increase the stability of gas film and to improve the repeatability and localization of ECDM micro-holes.

Keywords: ECDM; electrolyte damping and confinement effect; stable gas film; micro-holes array

1. Introduction

Glass is frequently applied in a variety of micro-electro mechanical system (MEMS) and microfluidics applications due to its desirable material characteristics, such as optical transparency, high electrical and chemical resistance [1]. Additionally, the glass has low signal losses due to its exceptionally high resistivity, making it an excellent substrates material for high radio-frequency applications. It should be noted that the requirement for the development of 3D connecting techniques such as through-glass vias (TGVs) is the fabrication of through-hole arrays on the glass substrate [2]. These materials must be micromachined in a repeatable, dependable, and cost-effective approach for practical applications. Although plasma etching, laser drilling and abrasive jet machining have been employed to fabricate micro-holes arrays in glass materials, these well-known techniques had

significant limitations [3]. More recently, Pandey et al. [4] fabricated a large aspect ratio through-holes arrays (<250 μm size) in a 1.1 mm thick glass substrate by ultrasonic machining, and it has a relatively high processing efficiency. Compared to these methods to fabricate micro through-holes arrays, electrochemical discharge machining (ECDM) is also comparatively inexpensive, and requires no costly infrastructure [5]. The method of machining micro holes on glass by ECDM was first reported as early as 1968 [6]. Recent explorations in micromachining have concentrated on ECDM, which has emerged as a viable alternative approach for micromachining glass materials due to its low cost, process flexibility, and relatively superior surface properties [7].

In the ECDM, arrayed tool electrodes or a single tool electrode are the two most frequent ways to fabricate micro through-hole arrays. Kannojia et al. [8] fabricated an array of 3×3 micro-electrodes for ECDM, and successfully machined a micro through-hole array in 520-μm-thick fused glass substrate. Despite the fact that electrode arrays offer a relatively higher machining speed, the issues of processing stability and low dimensional precision of the micro-holes cannot be addressed. Furthermore, gas bubbles become trapped between the electrode tips, causing an unstable electrochemical discharge that damages the holes arrays [9]. Consequently, the sidewalls of micro-holes were likewise fused together. In a few extreme cases, the glass substrate was broken during processing due to the immense stress created by the collapse of the bubbles. Although extending the spacing between the electrode tips reduces the chance of bubbles entrapped, the pitch size will be affected, resulting in undesirable effects in high density packaging applications [9]. Additionally, manufacturing of array micro tool electrodes will be costly and time consuming.

On the other hand, employing a single tool to fabricate a micro-hole array, not only simplifies the tool manufacturing process, but also increases the stability of the ECDM process. More recently, Arab

et al. [10] fabricated the micro-hole arrays of 91 micro through-holes (with an entrance average diameter of 411 μm) on 400-μm-thick glass wafer using a single tool. However, it should be noted that the geometric deteriorations (such as the large entrance overcut and HAZ of micro-holes) commonly occurs in the workpiece due to the stray electrochemical discharge (i.e. stray thermal energy) [7]. To overcome this issue, Zheng et al. [11] used flat sidewall–flat front tool to reduce sidewall discharge energy, and hence decrease the entrance overcut and HAZ of micro-holes. Chen et al. [12] developed an auxiliary nozzle that produces a coaxial jet was produced. This keeps the tool electrode submerged in electrolyte in the ECDM area at a low level, result in the electrochemical discharge is concentrated on the contact surface of the tool electrode tip and the glass workpiece material to be processed. Thus, the entrance overcut and HAZ of micro-holes were reduced accordingly. Most recently, Appalanaidu et al. [13] employed the glass substrate acted as a sacrificial layer for the stray thermal damages and left the glass workpiece material with minimal deterioration. As a result, the micro-hole overcut was reduced by 71.5%. Nonetheless, employing the glass substrate bonded over work material acted as a sacrificial layer will be burdensome and an additional issue. Moreover, it should be noted that the unstable gas film is also one of the main reasons for the stray electrochemical discharge in the ECDM [5]. Huang et al. [14] reported that the unstable gas film has an essential impact on the overcut, HAZ width, and especially dimensional uniformity precision of micro-holes. In general, the mean variance of several drillings in identical conditions is about 20 μm [15], whereas the radial overcut of the machined hole is in the range of 100–300 μm in the ECDM [16]. Therefore, it is a big challenge to achieve a minimal geometric deterioration and a high uniformity-precision of micro-holes array due to the unstable gas film. Furthermore, it should be noted that variations in the size of the micro-holes array also severely impact the Kelvin resistance of the TGV, significantly affecting their electrical

89 characterization [8].

90 Consequently, many efforts have been used to increase the stability of gas film during the ECDM
91 process [7]. Yang et al. [17] stated that a spherical tool electrode has a more stable gas film than that of
92 typical cylindrical tool electrode. When the tool electrode tip is spherical, the drilled entrance diameter
93 of micro-hole is decreased by 65%, and the extent of the HAZ is also reduced. Nonetheless, the
94 manufacture of spherical tool electrodes will be an additional issue that requires more attention.
95 Moreover, Singh et al. [18] observed that ultrasonic assistance could facilitate the formation of a stable
96 gas film over the tool electrode, simultaneously lowering the overcut and HAZ of the micro holes.
97 However, as according to Elhami et al. [19], the injection of intense vibrating amplitudes that exceed a
98 specific limit might cause serious disturbances in the gas film and electrolyte, and hence, leading to
99 unanticipated or uncontrolled occurrences. On the other hand, Jiang et al. [20] developed a theoretical
100 model and also conducted experimental research on the gas film in the ECDM process. According to
101 the established model, the electrolyte characteristics also impact the stability of gas film. In general, the
102 electrolyte additives represent a simple method to adjust electrolyte characteristics [21]. For instance,
103 Sabahi et al. [22] reported that when a mixed (NaOH + KOH) electrolyte is utilized, the gas film is
104 more stable than when the components are used separately. In another publication, Sabahi et al. [23]
105 employed sodium dodecyl sulfate and cationic surfactant cetyltrimethylammonium bromide electrolyte
106 additives to form a stable gas film by adjusting the physicochemical characteristics of the electrolyte.
107 Furthermore, Kunieda et al. [24] discovered that an oil dielectric with a high viscosity might reduce the
108 shocks caused by the damping effect in electrical discharge machining. Recently, as compared to
109 conventional electrolytes, i.e., KOH or NaOH which are Newtonian fluid electrolyte with a low
110 viscosity, non-Newtonian fluids of high viscosity are shown to provide a greater damping effect [25].

Inspired by this, in our previous work, Zou et al. [26] introduce for the first time a non-NTF electrolyte to increase the stability of gas film, and to achieve a complex microchannel with a spacing of 30 μm. Therefore, the present study aims to further employ a non-NTF electrolyte to ECDM to achieve high uniformity-precision and quality micro-holes array and to understand its mechanisms.

2. Experimental design

2.1. Materials

Polyacrylamide (PAM) is a conventional thickening agent, and its aqueous solution exhibits non-Newtonian behavior [27]. In our previous work, cationic Polyacrylamide was mixed to the KOH electrolyte 25wt%, which is a non-NTF electrolyte [26]. The non-NTF electrolyte used has concentrations of 0.1, 0.3, 0.5, 0.7, and 0.9 wt%, respectively. In addition, the tool electrode has a diameter of 0.2 mm and is made of tungsten carbide, whereas the anode electrode is a graphite plate (3 × 40 × 50 mm^3), and the 300-μm-thick soda lime glass substrate was chosen as the workpiece. The electrical conductivity of the non-NTF electrolyte was measured by a conductivity meter (ST2242, Jingge Electronics Co., Suzhou), the thermal conductivity was determined using a thermal conductivity meter (LFA447, NETZSCH Instrument Manufacturing Co., Germany), and the surface tension was recorded by a surface tension meter (DCAT21, Dataphysics., Germany). The measurement results are listed in Table 1. Furthermore, the critical point of the non-NTF electrolyte is approximately 0.1 wt%.

Table 1. The properties of non-NTF electrolyte.

Various concentrations of non-NTF electrolyte (wt%)	Electrical conductivity (KS/m)	Thermal conductivity (W/(m·K))	Surface tension(mN/m)
0 (i.e. KOH electrolyte 25wt%)	0.0602	0.824	85.52
0.1	0.0596	0.658	49.31
0.3	0.0531	0.653	47.69
0.5	0.0526	0.649	45.17
0.7	0.0548	0.643	41.73
0.9	0.0557	0.634	37.59

2.2. Experimental setup and parameters

It can be seen from Fig. 1a, the electrochemical discharge and high-temperature chemical etching remove material from the glass surface [7]. In general, the OH radicals from the electrolyte attach to the glass surface and eventually diffuse into the silicon oxide glass bonds, resulting in material chemical etching removal during the machining operation [28] (Fig. 1a). Moreover, Fig. 1b-d shows the schematic of the setup. The setup comprises a high-speed camera (FASTCAM SA-Z&200K-M-8Gb, Photron., Japan) and DC power supply. Among them, each axis of the stage is adjustable with a resolution of 1 μm. The spindle with a speed range of 0-2000 rpm. In the present work, micro-holes were drilled using a gravity-feeding device. This apparatus fed the tool electrode and maintained contact with the workpiece glass until the micro-through-holes were completely drilled. Furthermore, the gap between the tool electrode(cathode) and counter electrode (anode) is maintained at a distance of approximately 50 mm.

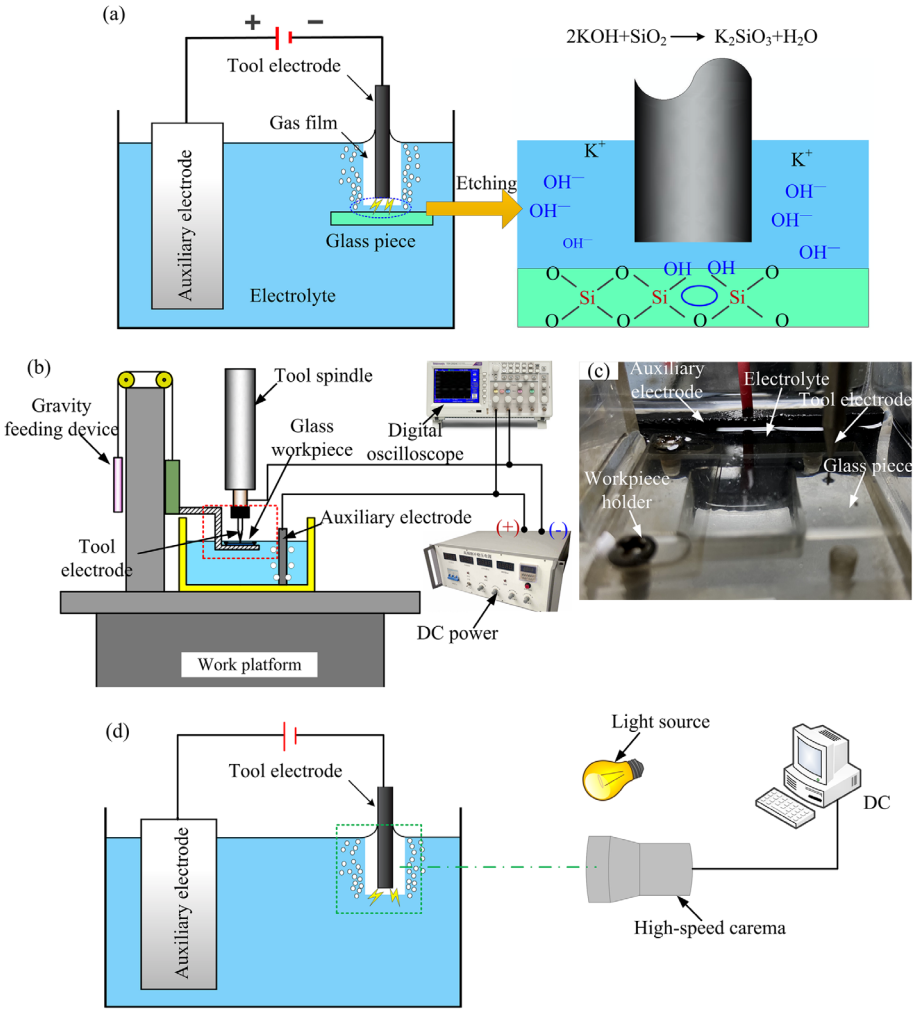

Fig. 1. (a) and (b) Schematic of ECDM process and ECDM experimental setup, (c) actual ECDM setup, and (d) schematic of high-speed camera setup.

In this experimental investigation, the comparison experiment was investigated. The high-speed camera was used to observed the dynamic properties of the gas film and the electrochemical discharge. The effects of voltage, electrolyte type and concentration, and tool rotation speed on the entrance overcut, and HAZ of micro-holes were evaluated by experiments. Each experiment is repeated 5 times and the results were averaged. The details of the experimental conditions are listed in Table 2. Moreover, the machining parameters (e.g., non-NTF electrolyte concentration, voltage and tool rotation speed.) were also optimized and the micro through-hole array was fabricated in the glass wafer.

158 **Table 2.** Machining parameters for experiments.

Process parameters	Values
Electrolyte	KOH, non-NTF electrolyte
KOH electrolyte (wt%)	25
non-NTF electrolyte (wt%)	0.1, 0.3, 0.5, 0.7, 0.9
Tool rotation speed (rpm)	200, 400, 600, 800, 1000 rpm
Voltage (V)	26, 28, 30, 32, 35

159

160 *2.3. Features of machined micro through-holes*

161 The diameter, overcut of micro-holes were measured by the confocal microscope (OSL400,
162 Olympus., Japan). The SEM (S3400N, Hitachi., Japan) observed the surface of the glass workpiece of
163 the micro-holes. In general, the nano-indentation can be used to measure the HAZ [23]. However, it
164 would not be feasible to carry indentation tests due to a thin glass wafer that is brittle and susceptible to
165 breaking. Consequently, the HAZ was described by determining the width of the thermally damaged,
166 unmachined outside perimeter of the through-hole entrance in this investigation (Fig. 2). The micro-
167 hole radial overcut $D_{overcut}$ can be calculated by:

168 $$D_{overcut} = R - r \quad (1)$$

169 where R is the radius of top-hole, r is the tool electrode radius.

170

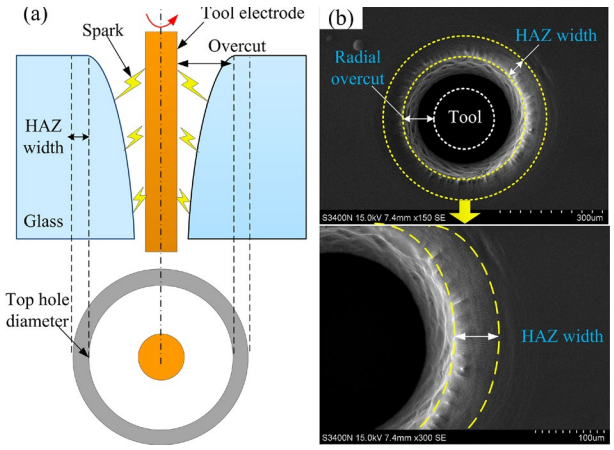

Fig. 2. (a) Schematic of the HAZ and entrance overcut of micro-hole, (b) the SEM image of the micro-hole.

3. Results and discussions

3.1. The electrochemical discharge characteristics with and without the damping and confinement effect

It is well known that the gas film's stability affects the geometric properties of micro-holes [29]. Thus, the dynamic properties of the gas film were investigated in order to establish a correlation the discharge activities with and without the damping and confinement effect (i.e. the conventional KOH electrolyte and non-NTF electrolyte). In this study, a series of images of an electrochemical discharge process were captured by high-speed camera. The voltage, electrode immersion, and frame capture rate fixed at 30 V, 2 mm, and 10000 fps, respectively. Fig. 3 shows that the conventional KOH electrolyte produced a thicker gas film than that of the non-NTF electrolyte. Furthermore, the gas film fluctuates frequently and randomly in the conventional KOH electrolyte [26] (Fig. 3a). As mentioned earlier, the non-Newtonian fluids can provide a greater damping effect than in Newtonian fluids [25]. The non-NTF electrolyte was also shown to be able to damp the discharge shock and constrain the gas film fluctuation (Fig. 3b). This can help to increase the repeatability and localization of ECDM micro-holes.

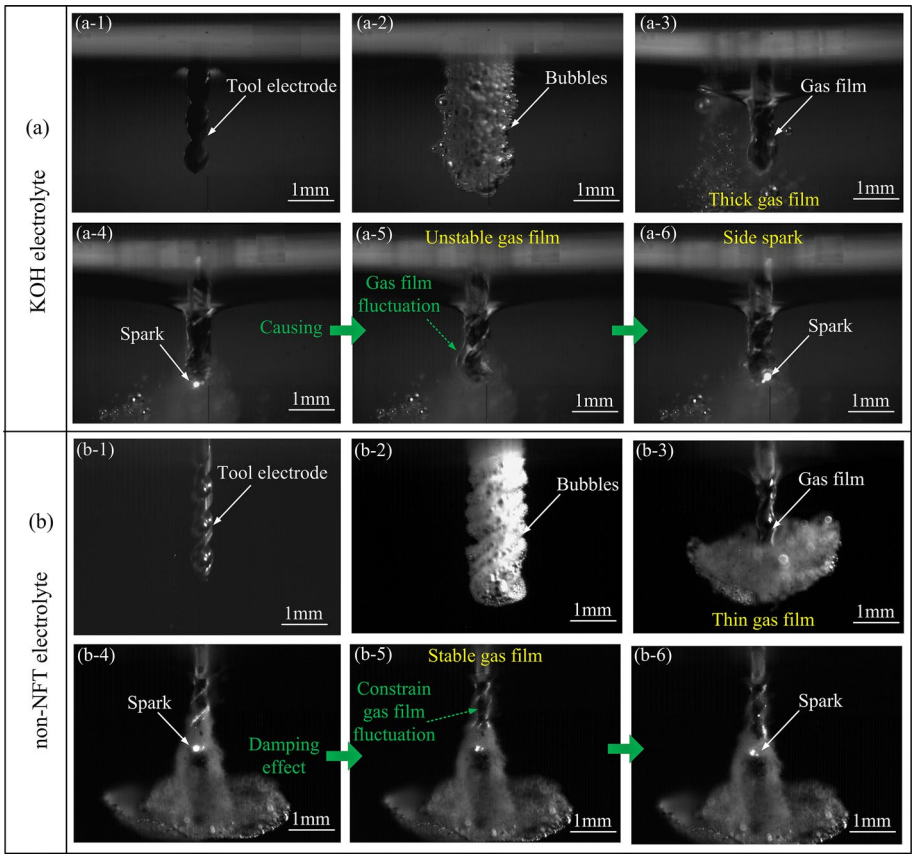

189

190 **Fig. 3.** Effect of electrolyte on electrochemical discharge process: (a) KOH electrolyte 25wt%, and (b)

191 non-NTF electrolyte 0.5wt%.

192

193 *3.2. Effect of the damping and confinement effect on the micro-holes*

194 To further illustrate the effect of the damping and confinement effect on the micro-holes, a

195 comparative experiment was conducted at different electrolyte (i.e. the non-NTF electrolyte

196 concentration of 0.3 wt%, the conventional KOH electrolyte concentration of 25 wt%,) and varying

197 voltages of 26, 28, 30, 32 and 35 V; keeping other parameters constant and the rotation speed of 600

198 rpm, and the fabrication micro-holes results are shown in the Figs. 4 and 5. Fig. 4 shows the

199 dimensions of fabricated micro-holes (i.e. hole radial overcut, and HAZ width), and Fig. 5 shows the

200 SEM images of micro-holes. It should be noted that a higher voltage resulted in a greater thermal

201 energy release, leading to the formation of a larger overcut and HAZ width around the hole's rim [5].

As a result, the micro-hole overcut and HAZ width were observed to increase as the voltage increased. However, in the conventional KOH electrolyte, with the voltage raised from 26 V to 35 V, micro-hole overcut increased from 135.6 to 167.3 μm and the HAZ width increased from 42.8 to 75.6 μm. In contrast, in the non-NTF electrolyte, the overcut increased from 61.7 to 146.6 μm and the HAZ width increased from 12.8 μm to 26.6 μm (Fig. 5).

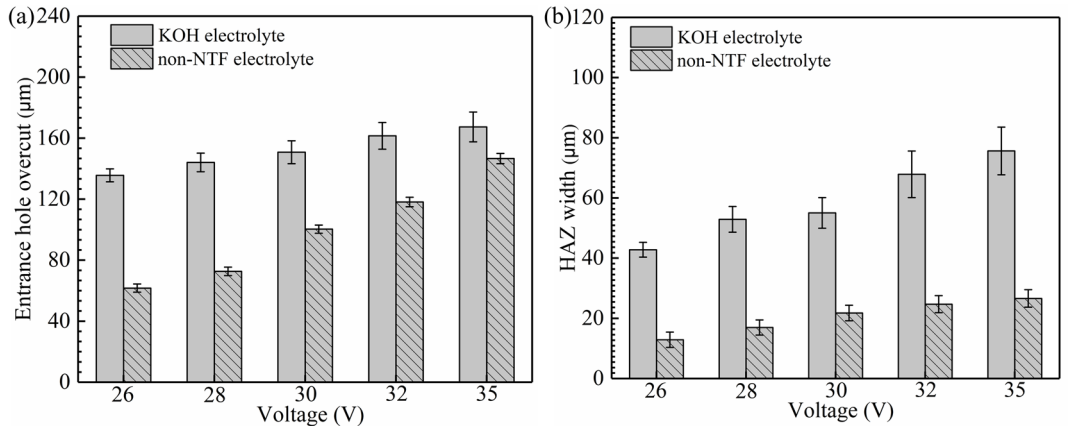

Fig. 4. Geometric characteristics of micro-holes: (a) top hole radial overcut, (b) HAZ width.

As discussed earlier, the stable gas film can decrease the stray electrochemical discharge, and hence, resulting in reducing overcut and HAZ width [30]. Compared to the non-NTF electrolyte, the gas film is unstable and thick in the conventional KOH electrolyte. This causes stray electrochemical discharge near micro-hole entrances. Thus, in the KOH electrolyte, both the overcut and HAZ width of the micro-holes were larger than in the non-NTF electrolyte. Furthermore, it can be evident from Fig. 5a, that increasing the voltage, a severe HAZ being generated around the rim of the micro-hole. However, there were less HAZ and the rim of the micro-hole surface was smooth in the non-NTF electrolyte (Fig. 5b). It should be noted that the overcut and HAZ width refer to the localization of ECDM. The larger overcut and HAZ width, the lower localization of ECDM. On the other hand, the standard deviation of overcut is 9.79 μm at the voltage of 35 V in the conventional KOH electrolyte. In contrast, the standard deviation is only 3.34 μm in the non-NTF electrolyte, and the deviation refers to

the repeatability of ECDM. Similarly, the larger deviation, the lower repeatability of ECDM. These results illustrate that the fabricated area is well constrained, significantly improving the localization and repeatability of ECDM micro-holes due to the damping and confinement effect.

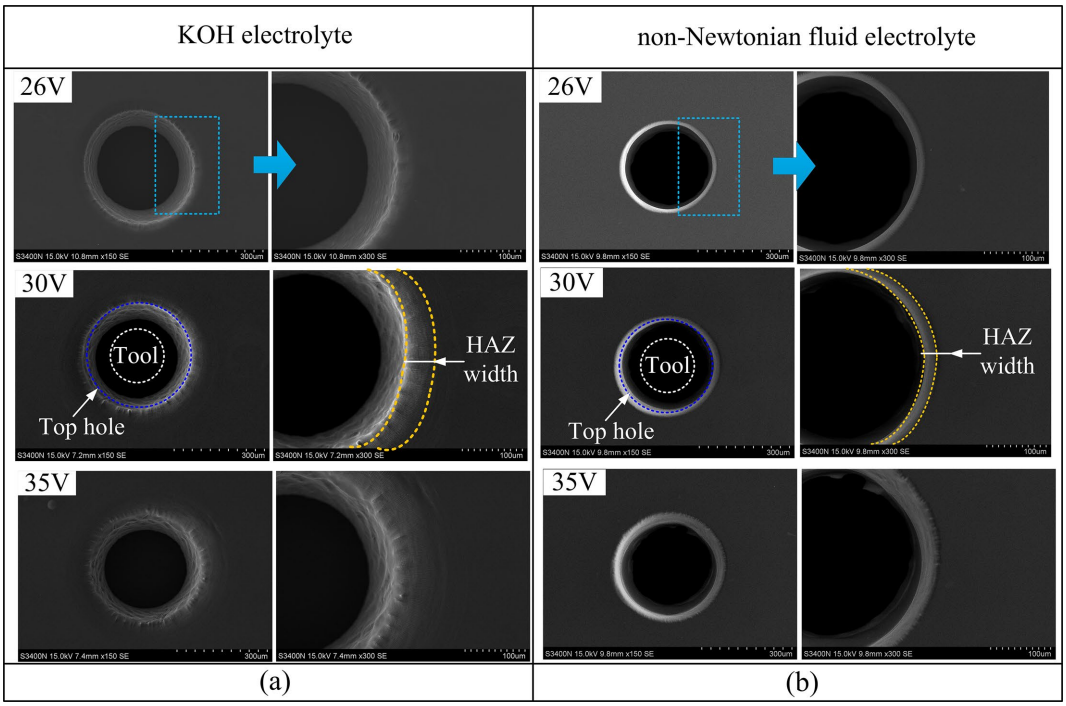

Fig. 5. SEM of the micro-hole fabricated using different electrolyte: (a) KOH electrolyte, (b) non-NTF electrolyte.

To further study the HAZ, the EDS analysis of the oxygen content of the HAZ surface in different conditions were also conducted. As shown in Fig. 6, the oxygen content of the machined surface with conventional KOH electrolyte (49.87 wt%) is higher than that of non-NTF electrolyte (40.81 wt%) and the unmachined glass surface (36.49 wt%). The increase in the oxygen content of the machined surface, implies the more severe HAZ. Thus, this result further indicates that using the non-NTF electrolyte can produce a smaller HAZ than in the conventional KOH electrolyte.

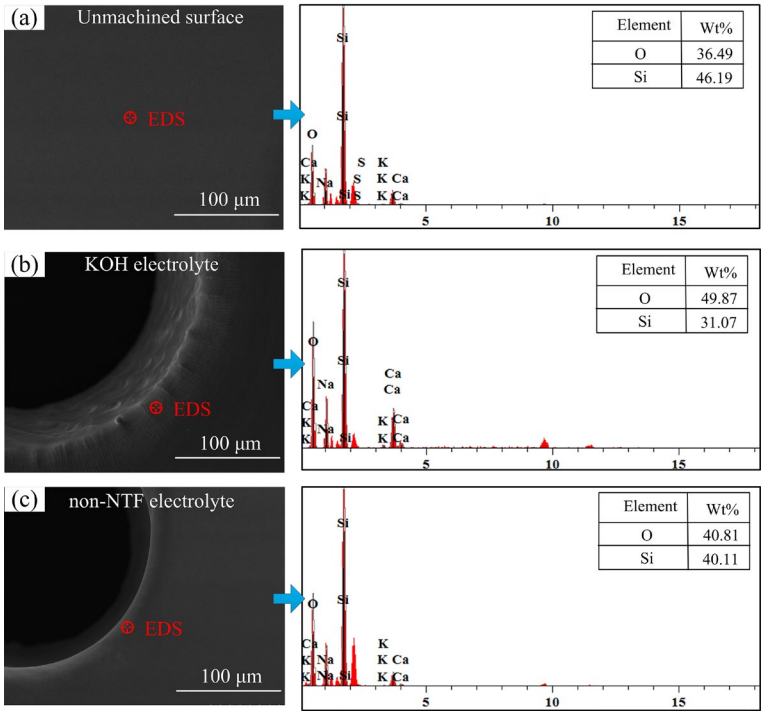

232

233 **Fig. 6.** EDS analysis results of machined surface in different conditions: (a) unmachined surface, (b)

234 the KOH electrolyte, and (c) the non-NTF electrolyte.

235 The SEM images of the machined inner wall and exit of the micro-holes are shown in Fig. 7. In

236 the conventional KOH electrolyte, the machined inner wall of the micro-holes reveals a fractured

237 surface and there are surface defects of material spalling and micro cracks at the hole exit (Fig. 7a and

238 b). In general, due to the load between the electrode and the workpiece under gravity-feed machining

239 and the brittle nature of the thin glass substrate, the stress results in a direct damage to the glass

240 substrate at the micro-hole exit [17]. However, it can be seen from the Fig. 7c and d, the machined

241 inner wall of the micro-holes is a smooth surface and there no visible cracks near the hole exit in the

242 non-NTF electrolyte. As discussed earlier, the non-NTF electrolyte can provide a continuous and stable

243 discharge [26]. Consequently, a more uniform softening effect is available in the drilling area of brittle

244 glass substrate. Compared with KOH electrolyte, the surface damage caused by the stresses developed

245 during the machining process can be reduced in the non-NTF electrolyte. Thus, in the non-NTF

electrolyte, there no visible cracks near the hole exit.

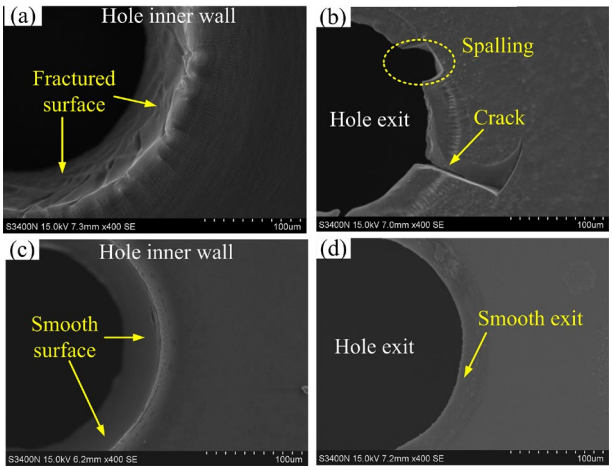

Fig. 7. (a) and (b) the machined inner wall and exit of the micro-holes in KOH electrolyte, (c) and (d) the machined inner wall and exit of the micro-holes in non-NTF electrolyte.

On the other hand, a thick and unstable gas film will be producing an unstable and high-intense electrochemical discharge [18]. Consequently, thermal stresses are generated, and an uneven heating and cooling of the material occur in the localized zone. This heat energy over the machined surface caused the thermal expansion in the localized region and simultaneously developed the thermal gradient in the machined zone. When the thermal gradient over the fracture strength value, the material fractured in a localized zone and generated a crack [31]. Thus, this may be able to lead to the machined inner wall of the micro-holes is a fractured surface in the conventional KOH electrolyte (Fig. 7a and b). In comparison, the electrolyte damping and confinement technique can provide a continuous and stable discharge [26]. This electrochemical discharge conditions can avoid the uneven heating and cooling of the material in the localized zone, resulting in a reduction of the thermal expansion as well as thermal gradient in the localized region. Thus, in the non-NTF electrolyte, the machined inner wall of the micro-holes is a relatively smooth surface. As a result, the stress and thermal play a significant in the damaged surface during ECDM process.

Based on the above discussions, Fig.8 further illustrates the process schematic of the ECDM with and without the electrolyte damping and confinement effect. As mentioned previously, in the ECDM process, the thermal variations and shocks directly affect the electrolyte in the boundary of the gas film [32]. Thus, the gas film in the conventional KOH electrolyte (i.e. without damping and confinement effect) is fluctuating (Fig. 8a). This causes a stray electrochemical discharge near the entrance of micro-holes on the glass wafer, and as a consequence, resulting in increasing the severity of overcut and HAZ (i.e. decreasing the localization of ECDM). On the other hand, the structure of the gas film fluctuates frequently and randomly, decreasing the machining dimensional accuracy of micro-holes array (i.e. reducing the repeatability of ECDM). Therefore, drilling a high uniformity-precision and quality micro-holes array on glass is a big challenge in the conventional KOH electrolyte. In contrast, Fig. 8b shows the ECDM utilizing a non-NTF electrolyte (i.e. with damping and confinement effect). Compared to the traditional KOH electrolyte, the non-NTF electrolyte is not only able to damp the electrochemical discharge shock, but also constrain the gas film (i.e. increase the gas film's stability). Consequently, increasing the localization and repeatability of ECDM micro-holes, and a high uniformity-precision and quality micro-holes array can be achieved. In order to understand the electrolyte damping and confinement technique, more experimental investigations were conducted and their results are presented in the next sections.

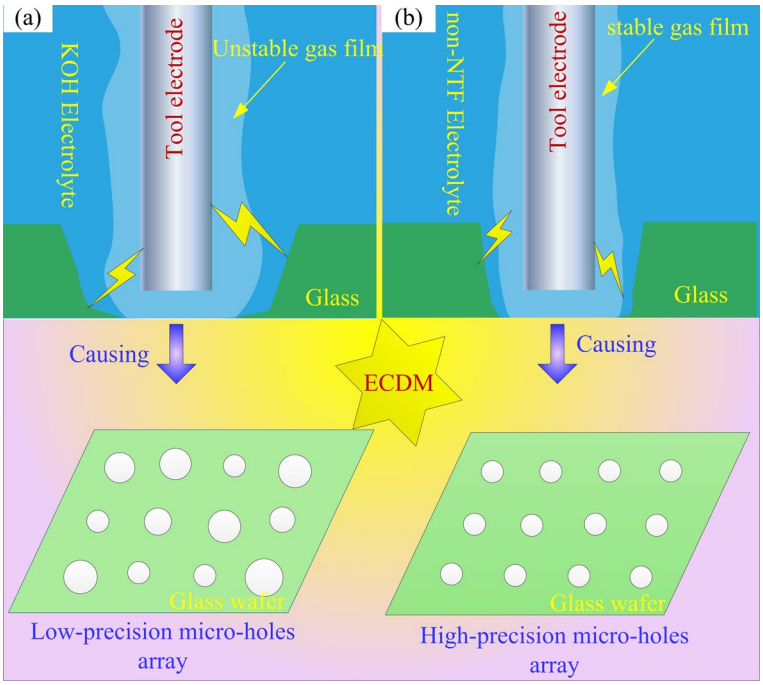

Fig. 8. Schematic of the effect of the damping and confinement effect on the micro-holes.

3.3. Effect of the non-NTF electrolyte concentration

The damping and confinement effect has a significant impact on the micro-holes, as demonstrated in section 3.2. In generally, the non-NTF electrolyte concentration has an essential role in damping and confinement effect. Therefore, to further investigate, micro-holes were fabricated with different electrolyte concentration (wt%) of 0.1, 0.3, 0.5, 0.7 and 0.9, whilst the voltage and rotation speed fixed at 30 V and 600 rpm, respectively. The fabricated results are shown in Figs. 9 and 10. It can be observed that with the electrolyte concentration increasing from 0.3 wt% to 0.5 wt%, the overcut decreased from 118.3 μm to 89.4 μm, and the HAZ reduced form the 26.3 μm to 20.6 μm. Further increase the concentration from the 0.5 wt% to 0.9 wt%, while the overcut increased from 89.4 μm to 126.5 μm, and the HAZ rasied form the 20.6 μm to 71.7 μm. Obviously, under either the low (i.e. 0.1wt%) or high concentrations (i.e. 0.9wt%), the geometrical properties of the fabricated micro-holes cannot be expected. In particular, at a concentration 0.9 wt%, a severe HAZ occurs at the micro-hole

rim (Fig. 10c). However, the micro-hole rim is smooth with a concentration of 0.5wt% (Fig. 10b). Furthermore, the corresponding standard deviation first decreased as the concentration increased from 0.3 to 0.5 wt%, while increased with the further increase in concentration.

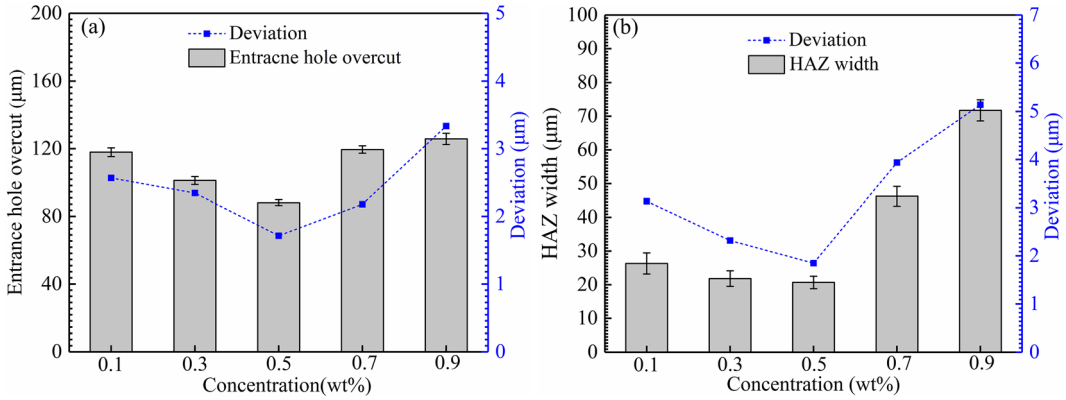

Fig. 9. Effect of the non-NTF electrolyte concentration on the (a) radical overcut, (b) HAZ width.

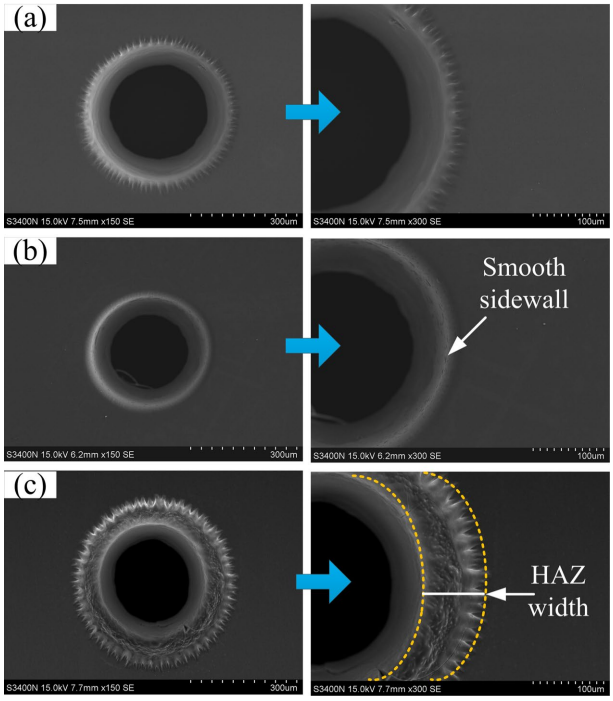

Fig. 10. SEM of the through-hole machined by different non-NTF electrolyte concentrations: (a) 0.1 wt%, (b) 0.5wt%, and (c) 0.9 wt%.

The reason for the change of geometric characteristics of micro-holes with different non-NTF electrolyte concentrations can be explained as follows: (i) In general, the damping force is proportional to viscosity of the fluid [33], and the viscosity increased with the non-NTF electrolyte concentration

(Fig. 11). This resulting in an increased damping force, and hence, enhancing the damping and confinement effect of non-NTF electrolyte. That is to say, as increasing the non-NTF electrolyte concentration, the damping and confinement effect increasing accordingly. Furthermore, Fig. 12a illustrates that, at a concentration of 0.1wt%, the damping effect too low to sufficiently reduce the electrochemical discharge shock. As a result, there are severe electrolyte turbulence and frequent gas film fluctuations (Fig. 12a), and as a consequence, fabrication of the micro-holes with a large overcut and HAZ at a concentration of 0.1wt% (Fig. 9). (ii) On the other hand, the movement of the bubbles were restricted when the viscosity was too high. That is to say, when damping and confinement effect is too large, it restricts the bubbles to move. It can be clearly observed that almost all the bubbles attached to the surface of the tool electrode and it produced a thick bubble and/or gas film with a concentration 0.9 wt% (Fig. 12b). Moreover, the electrolyte replenishment is affected and the bubbles accumulate at the micro-hole entrance (Fig. 12c). Which causes a severe stray electrochemical discharge on the micro-holes entrance [7]. Accordingly, a severe overcut and HAZ of micro-holes would occur at 0.9 wt%. Even, there are cracks at the entrance and the inner wall of the micro-hole due to the discharge concentration at the entrance of the hole maybe produce a high thermal gradient in the localized zone (Fig. 12c).

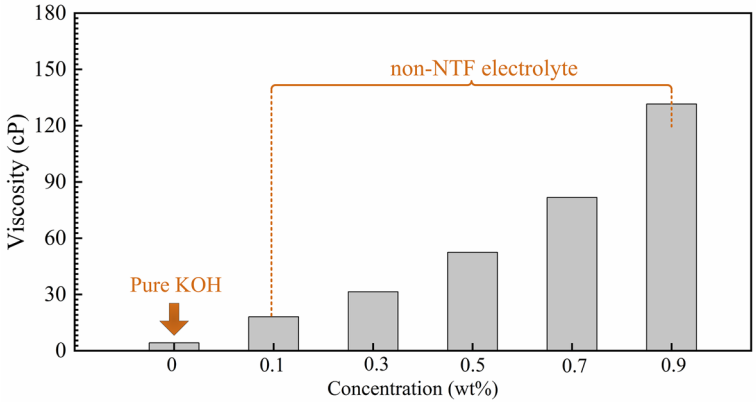

Fig. 11. The viscosity of different non-NTF electrolyte concentration.

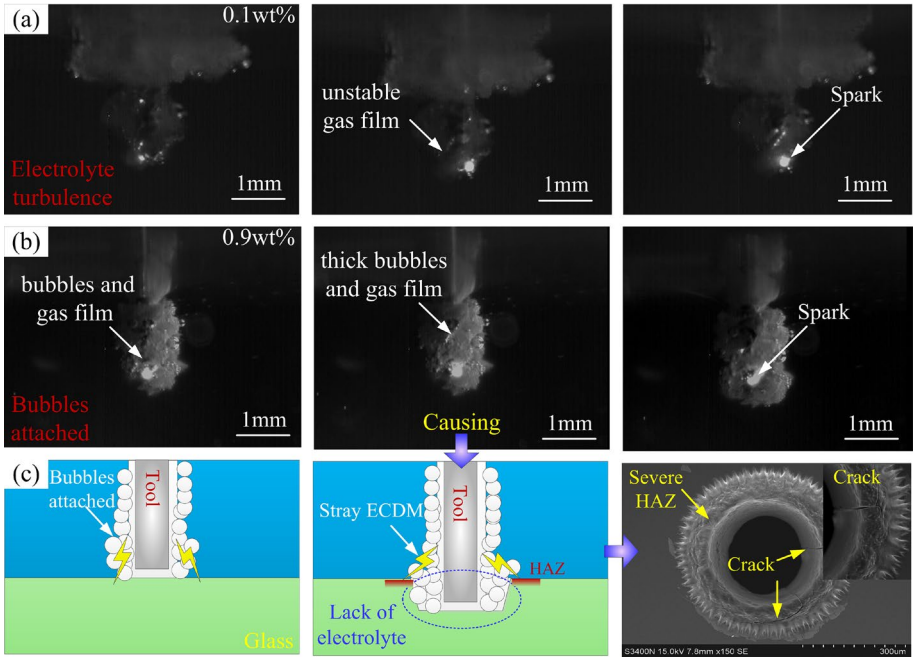

Fig. 12. (a) and (b) the high-speed camera picture of electrochemical discharge characteristics in the non-NTF electrolyte 0.1wt% and 0.9 wt%, respectively, and (c) the effect of the large non-NTF electrolyte concentration on the micro-holes.

3.4. Effect of the tool rotation speed

As discussed in section 3.3, the damping and confinement effect is greatly affected by the viscosity of non-NTF electrolytes. Moreover, the viscosity of the non-Newtonian fluid is typically proportional to the local strain rate [34]. It should be noted that the tool rotational speed has a direct effect on the local strain rate as well as viscosity. Therefore, to study the effect of different tool rotation speed on the geometric characteristics of micro-holes and damping and confinement effect. Micro-holes were processed at tool rotation speeds (rpm) of 200, 400, 600, 800 and 1000, while the electrolyte concentration and applied voltage were 0.5wt% and 30 V, respectively. The processed results are shown in Figs. 13 and 14.

As shown in Fig. 13, as the rotating speed increases, the overcut, HAZ width, and corresponding

deviation of the micro-hole decrease at first, but then increase over 600 rpm. For example, with the increase in rotational speed from 200 to 600 rpm, the overcut decreased from 107.4 to 87.9 μm and the HAZ width decreased from 24.1 to 19.7 μm. In general, the rotating electrode stirs the electrolyte, increasing its circulation. As a result, the gas film could be formed rapidly and stably, which contributed to the improvement of the geometric properties [5]. However, further increasing in rotational speed from 600 to 1000 rpm, the overcut increased from 87.9 to 117.1 μm, the HAZ width increased from 19.7 to 29.3 μm, and the corresponding standard deviation was increased accordingly. It is also evident from the Fig. 14, at rotational speed (rpm) of 200 or 1000, there is a severe thermal effect on the rim of the micro-holes.

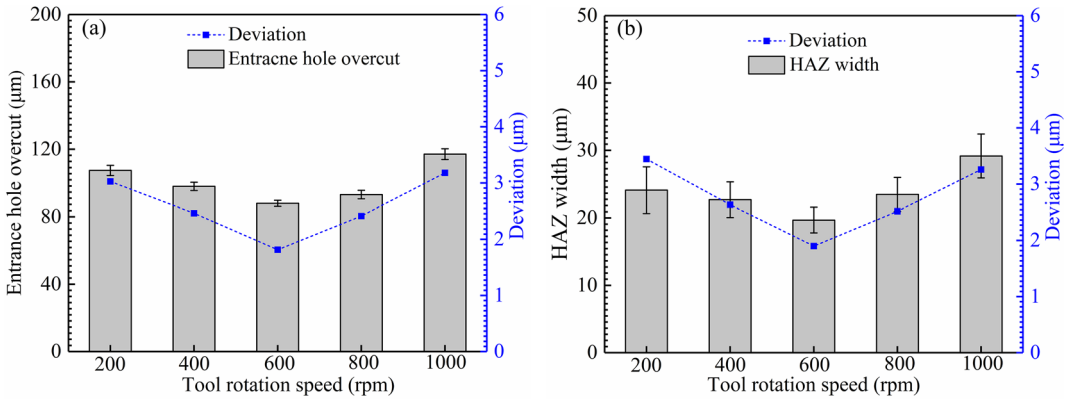

Fig. 13. Effect of tool rotation speed on the (a) radical overcut, (b) HAZ width.

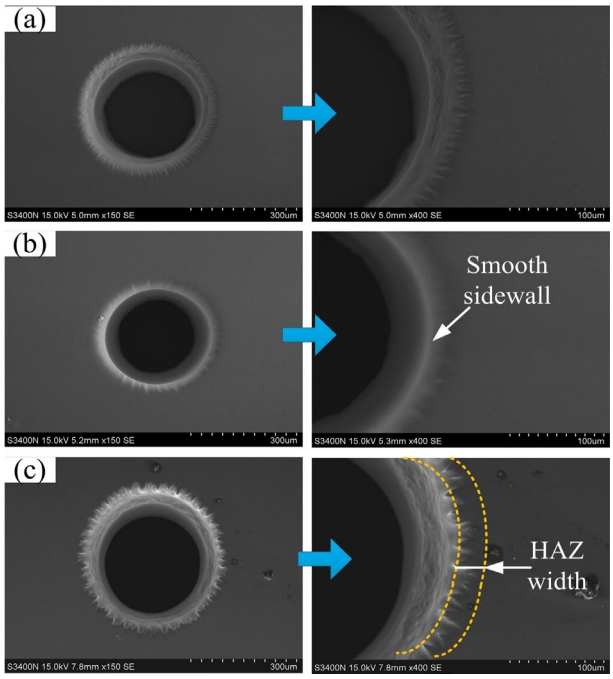

Fig. 14. SEM of the through-hole machined the glass substrate using different tool rotation speed:(a) 200 rpm, (b) 600 rpm, and (c) 1000 rpm.

This phenomenon may be caused by the rheological characteristics of non-Newtonian fluids. It is widely known that the viscosity of a non-Newtonian fluid is related to the local strain rate. In the present investigation, the rheological property is measured by a rheological meter (Malvern, kinexus ultra). Clearly, the proposed non-NTF electrolyte is a pseudo plastic fluid are shown in Fig.15. In general, the viscosity of the fluid can be calculated by:

$$\mu = \frac{\tau}{\gamma} \tag{2}$$

Where τ is the stress, γ is the shear rate. So, as the shear rate increases, the viscosity of non-NTF electrolyte reduces. That is to say, when the tool rotation speed is increased, the viscosity of non-NTF electrolyte is decreased, and as a consequence, the damping and confinement effect is reduced accordingly.

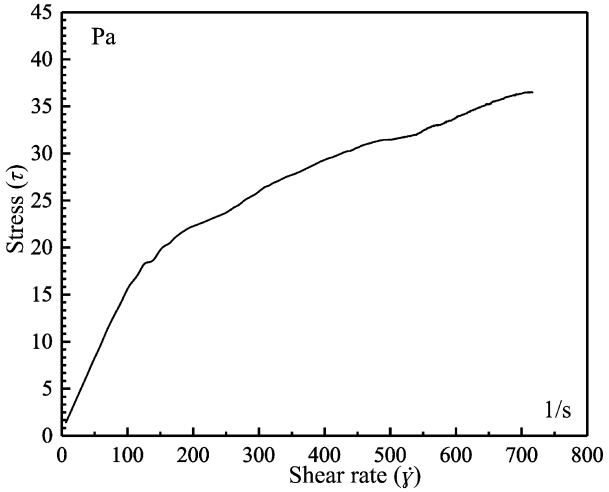

Fig. 15. The stress-strain curve of the non-NTF electrolyte.

Fig. 16 depicts the mechanism responsible for this phenomenon at low and high rotation speed. In the case of the low tool rotation speed, the viscosity of the non-NTF electrolyte is larger and the bubbles adhered to the tool electrode's surface and produced a thick bubble or gas film. Furthermore, the low tool rotation speed limits the electrolyte replenishment in the ECDM of the micro-holes area. This results in a severe stray electrochemical discharge on the micro-holes entrance, causing a severe overcut and HAZ at a low tool rotation speed (Fig. 16a). In contrast, the viscosity of non-NTF electrolyte is lower at high tool rotation speed. As discussed in section 3.3, the damping force is proportional to viscosity of the fluid [33]. As a consequence, it results in a reduction of the damping and confinement effect, and thus, decreases the stability of gas film. Thus, at a high tool rotation speed, there is also a severe stray electrochemical discharge on the micro-holes entrance (Fig. 16b).

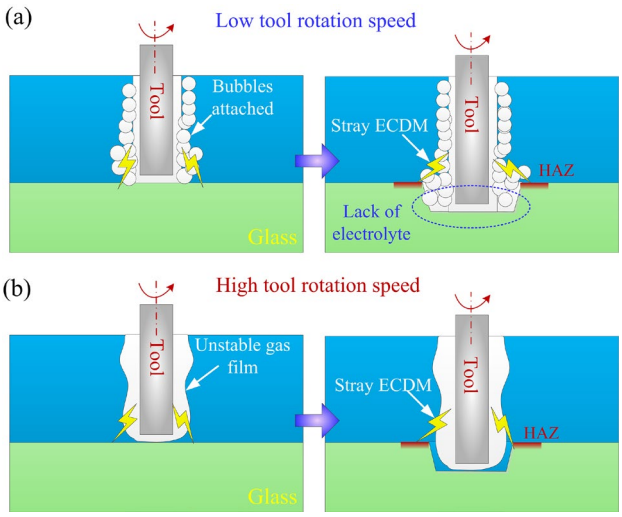

Fig. 16. Schematic of the effect of the different tool rotation speed: (a) low speed, and (b) high speed.

Fig. 17 a-f further provided evidence of the fact that the non-NTF electrolyte concentration and tool rotation speed have a significant effect on the damping and confinement effect and micro-holes. As shown in Fig. 17a, since the damping and confinement effect of non-NTF electrolyte 0.1wt% is relatively small at a low tool rotation speed of 200 rpm. As a result, the hole exit has material spalling issue. When further increase the tool rotation speed, the damping and confinement effect is greatly decreased, resulting in a severe overcut, HAZ and the hole exit of crack (Fig. 17b). Furthermore, at a low tool rotation speed of 200 rpm, when using the non-NTF electrolyte 0.5 wt%, the overcut and HAZ are larger than in non-NTF electrolyte 0.1 wt% (Fig. 17c). At a high tool rotation speed of 1000 rpm, the damping and confinement effect of non-NTF electrolyte 0.5 wt% is larger than that of non-NTF electrolyte 0.1 wt %, a relatively low overcut and HAZ can be achieved (Fig. 17d). In comparison, at a tool rotation speed of 200 rpm, when using the non-NTF electrolyte 0.9 wt%, the damping and confinement effect is too large. This results in a severe stray and high-intense electrochemical discharge on the micro-holes entrance, and as a consequence, causing severe overcut, HAZ and surface defect (Fig. 17e). Further increase the tool rotation speed (i.e. 1000 rpm), the damping and confinement effect of non-NTF electrolyte 0.9 wt% is also decreased accordingly. Thus, resulting in a relatively low

overcut and HAZ than that of the low tool rotation speed of 200 rpm.

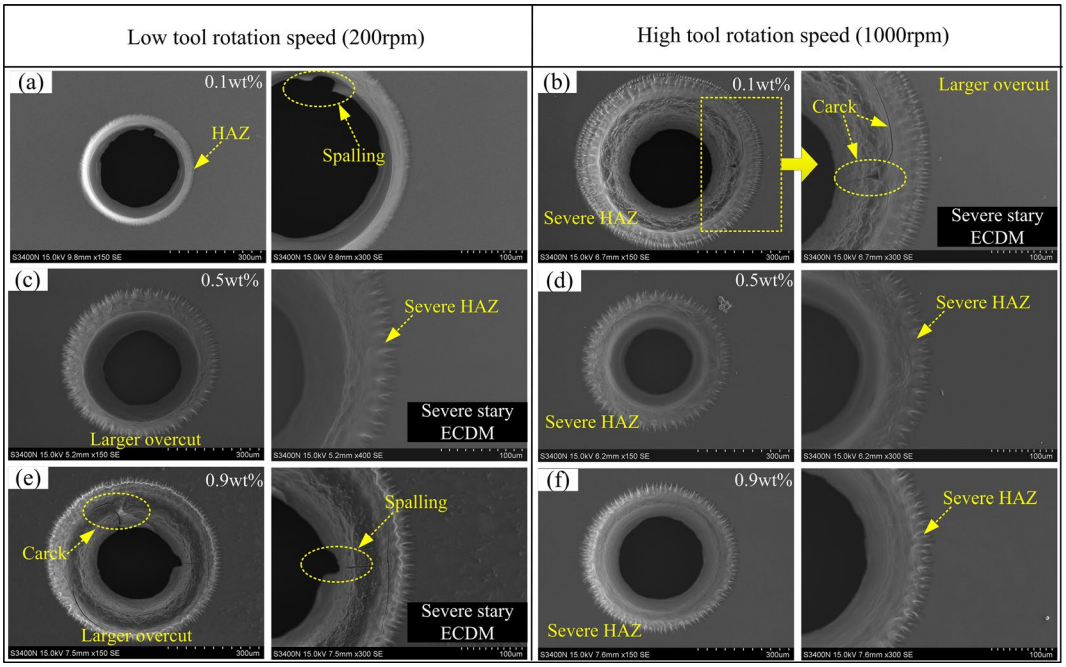

Fig. 17. The effect of the different tool rotation speed and non-NTF electrolyte concentration on the micro-holes.

These results further demonstrated that the non-NTF electrolyte concentration and tool rotation speed have an essential effect on the damping and confinement effect, significantly affecting the geometric properties of micro-holes. Based on the above discussions, within the range of investigated conditions, the produced damping and confinement effect under the non-NTF electrolyte 0.5 wt% and tool rotation speed of 600 rpm conditions were optimized for the process.

3.5. Tool electrode wear

It is well known that the tool electrode wear also has a significant impact on the dimensional uniformity of the micro-holes, particularly when fabricating a high-precision micro-holes array using a single tool electrode. Obviously, the tool wear should also be investigated prior to the micro-holes array processing. Thus, in this section, the tool wear was investigated. The fixed parameters were fabricated

with a 30 V voltage and 10 min machining time, while the tool immersion, KOH electrolyte, and non-NTF electrolyte concentration were fixed at 2 mm, 25 wt%, and 0.5 wt%, respectively. It can be observed from the Fig.18, the surface of the original tool electrode is coated. The tool electrode placed in the KOH electrolyte causes serious surface coating wear, and hence, exposes the base metal of the tool electrode (Fig.18b). In comparison, in the non-NTF electrolyte, the coating wear and base material exposure is much lower than that of the KOH electrolyte (Fig.18c).

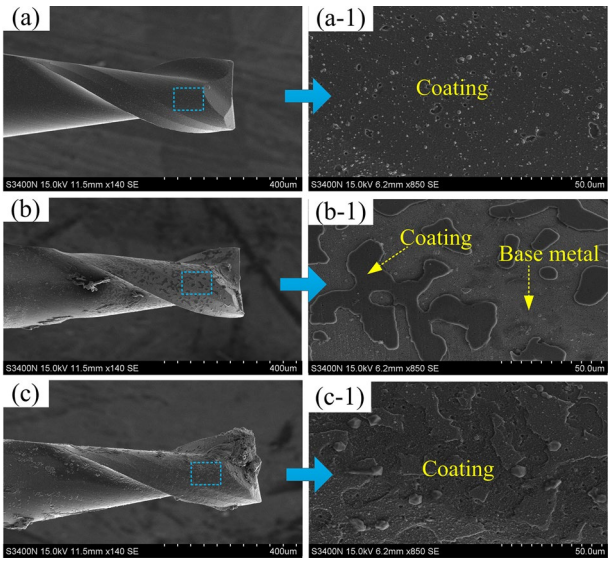

Fig. 18. SEM images of the tool electrode wear in different electrolyte: (a) original tool electrode, (b) KOH electrolyte, and (c) non-NTF electrolyte.

To corroborate previously, EDS and mapping analysis results of the tool electrodes was used to further study (Fig. 19). The coating of the original tool electrode consists of 85.5 wt% titanium (Ti) and smaller amounts of other elements. Because this coating is dense, the original electrode surface contains 5 wt% tungsten (W) (Fig. 19a). In contrast, when the conventional KOH 25 wt% was used, there was a significant increase in the W content and a reduce in the Ti content. Moreover, the results of the mapping analysis indicate that the Ti coating is destroyed, and the base material W is exposed (Fig. 19b). However, in the non-NTF electrolyte, the percentage of W and Ti on the tool surface are 67.1 wt%

and 5.2 wt%, respectively. In general, the change in electrode appearance, reduction of Ti coat, and the presence of the W element in the EDX analysis results were considered to be the criteria for electrode wear. Compared to the original tool electrode, the percentage of W and Ti of the tool surface used in the non-NTF electrolyte changes very little.

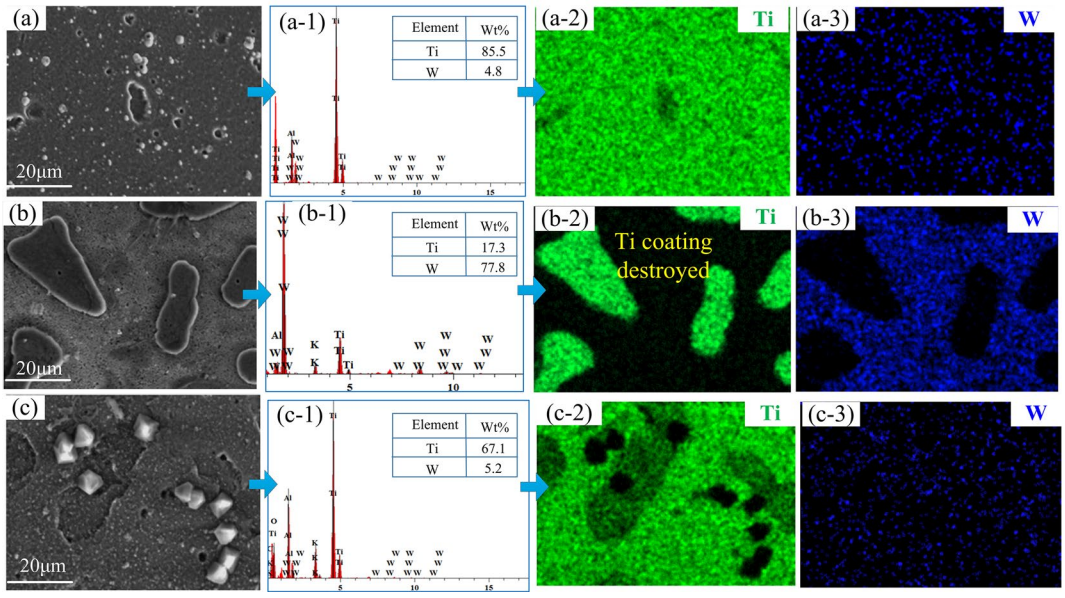

Fig. 19. EDS analysis results of tool electrodes in different electrolytes: (a) original tool electrode, (b) the KOH electrolyte, and (c) the non-NTF electrolyte.

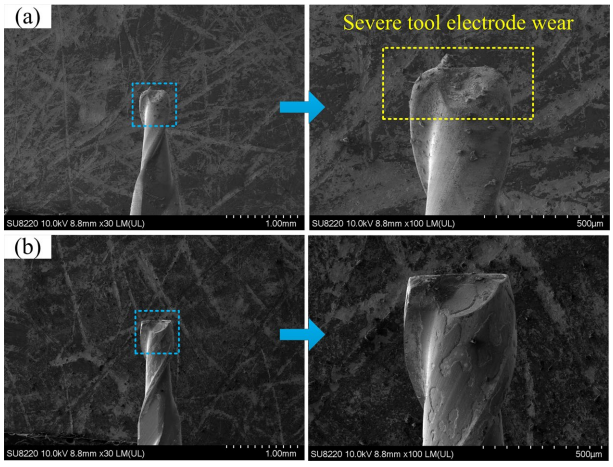

Fig. 20. SEM image of tool electrodes wear with a 30 min machining time: (a) KOH electrolyte, (b) non-NTF electrolyte.

The reason for the change of tool wear with and without the confinement effect can be explained

as follows: In general, a thick and unstable gas film will be producing a high-intense electrochemical discharge thermal energy [18]. As discussed earlier, compared to the KOH electrolyte, the non-NTF electrolyte can produce a more thinner and stable gas film [26]. Accordingly, the tool electrode will be subject to higher electrochemical discharge thermal energy in the KOH electrolyte. This causes serious surface coating wear, thus, exposes the base metal of the tool electrode (Fig.19b). As machining continues, more surface coating of the tool electrode is wear, resulting in further wear of the exposed tool electrode base metal material. In contrast, the non-NTF electrolyte can provide a relatively low-intense electrochemical discharge thermal energy, leading to the coating wear is much lower than that of the KOH electrolyte (Fig.19c). As a result, a lower tool wear can be obtained in the non-NTF electrolyte. Furthermore, when further increase the machining time (i.e. 30 min), the conventional KOH electrolyte has a much severe tool wear than in the non-NTF electrolyte (Fig. 20). As noted, the low electrode wear in the non-NTF electrolyte implies that it is advantageous for high-precision machining of micro-hole arrays with a single tool electrode.

3.6. Optimized process parameters for ECDM of micro through-holes array

As previously discussed, the results show that an applied voltage of 30 V, non-NTF electrolyte concentration of 0.5wt%, and tool rotation speed of 600 rpm is optimal when the overcut, HAZ and the dimensional uniformity of the micro-holes are the decisive factors. As depicted in Fig. 21, by using proposed non-NTF electrolyte and optimal parameters, a micro through-hole array was successfully fabricated on a 300-μm-thick glass substrate. Thermal and mechanical damage was observed to be minimal in the drilled holes.

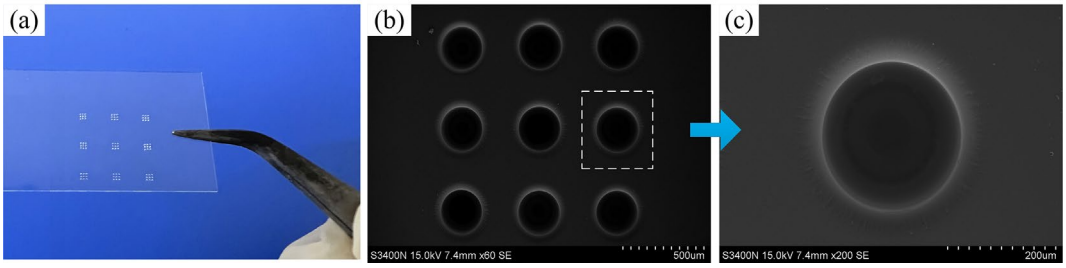

Fig. 21. Micro through-hole array machined using the optimum parameters: (a) optical image of a 300-μm thick glass substrate having a through-holes array, (b) SEM images of through-holes array, (c) SEM images of a single micro-hole.

Fig. 22 shows the measured results of the micro through-hole array. A total of 81 micro-holes were considered for measurement; the diameter of the micro through-hole on the top surface ranged from 336.5 μm to 349.8 μm (mean width = 343.8 μm), and the HAZ width ranged from 14.5 μm to 21.8 μm (mean width = 18.01 μm). In addition, it could be calculated that the standard deviation of the diameter and HAZ width of the micro through-hole was 3.47 μm and 1.52 μm, respectively, showing an excellent localization and repeatability of ECDM micro-holes.

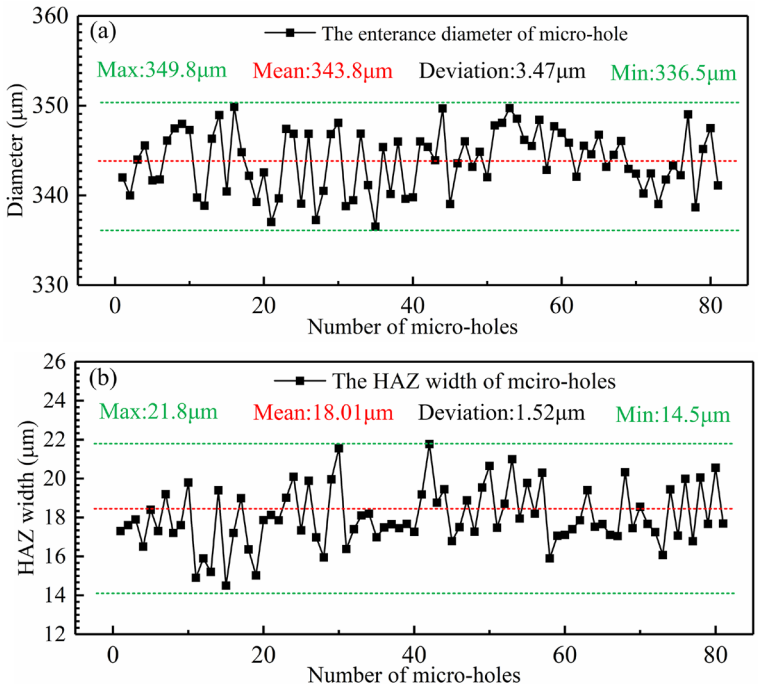

Fig. 22. Diameter and HAZ width of the micro through-hole on the top surface: (a) diameter, and (b)

HAZ width.

4. Formation of through-glass vias

Before the micro-hole arrays are filled with copper, the glass wafers were washed for 10 minutes with ethanol. After cleaning, the glass substrate was dried and then submitted to electrodeposition. Bottom-up electrodeposition was applied to ensure void-free filling of through-micro-hole arrays [10]. Firstly, as a conductive seed layer, a 200 μm-thick copper foil was bonded to a support glass wafer. Then, the glass wafer was electrodeposited using the $CuSO_4.5H_2O$ (200 g/L), H_2SO_4 (60 g/L), a purity copper anode, and electrolyte pumping device. A DC power supply (Edx electron, China) with a current of 50 mA was employed for the electrodeposition. Additionally, the seed layer on the back of the through-holes was required for the electrical characterization of the Kelvin structure. Polishing removed the remaining seed layer after completing. The confocal microscope was then performed to evaluate the quality of electro-deposition. The machined cross-section of a through-hole are shown in Fig. 23a. After 6 hours of electrodeposition, the through hole arrays was fully filled, as shown in Fig. 23b.

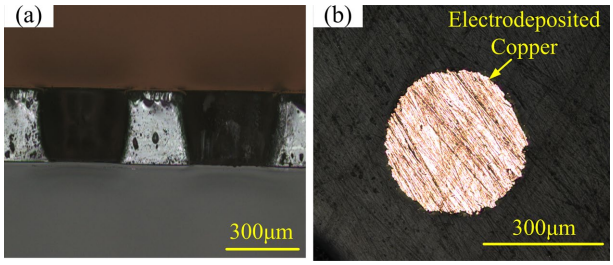

Fig. 23. Optical images showing: (a) cross-sectional view of the through-hole, (b) view of TGVs.

As discussed in earlier, variations in the size of the through-hole arrays alter the Kelvin resistance of the TGVs, hence influencing the electrical characterization of Kelvin TGVs [8]. This investigation is analyzing the manufacturing of through micro-hole arrays with a smaller size variation in order to

enhance the electrical characterization of Kelvin TGVs. To verify the stability of the electrical characterization of TGVs, its Kelvin resistance were tested. Fig. 24 shows the test results, the resistance of the TGVs ranged from 253 mΩ to 278 mΩ. In addition, the standard deviation of the Kelvin resistance of the TGVs was 5.35 mΩ. These results further indicate that the damping and confinement effect of a non-NTF electrolyte was able to effectively constrain the gas film fluctuations and a high uniformity-precision micro-hole arrays could be achieved.

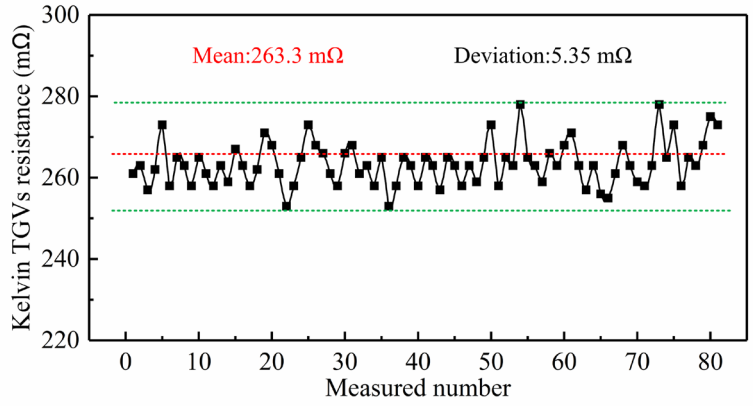

Fig. 24. Measurements of the Kelvin resistance of the TGVs.

5. Conclusions

This present work proposed a damping and confinement technique to increase the localization and repeatability of ECDM micro-holes. Based on the experimental results, the major conclusions are summarized:

(1) The high-speed camera observation results indicated that the gas film fluctuation was well reduced by the damping and confinement effect.

(2) Compared with the conventional KOH electrolyte, the repeatability and localization of ECDM micro-holes are significantly improved with the non-NTF electrolyte. The repeatability percentage improvement reached to 67.92 %, and the entrance overcut and the width of HAZ of micro-holes were

reduced about 43.84 %, and 64.81%, respectively.

(3) The non-NTF electrolyte concentration and tool rotation speed have an essential effect on the damping and confinement effect as well as geometric properties of micro-holes. When damping and confinement effect is too large and/or too low, it resulted in a severe overcut and HAZ of the micro-holes entrance. Within the range of investigated conditions, the produced damping and confinement effect under the non-NTF electrolyte 0.5 wt% and tool rotation speed of 600 rpm conditions were optimized for the process.

(4) By employing a non-NTF electrolyte, a minimal geometric deterioration and high uniformity-precision micro-hole arrays with average entrance diameter 343.8 μm and HAZ width 18.01 μm were successfully fabricated in the 300-μm-thick glass substrate. The standard deviations of hole entrance diameter and HAZ width were only 3.47 μm and 1.52 μm.

(5) It can be concluded that using the damping and confinement effect of non-NTF electrolyte can improve the localization and repeatability of ECDM the micro-holes. In addition, it is a promising approach with high potential for industrial applications.

CRediT authorship contribution statement

Zhixiang Zou: Conceptualization, Methodology, Writing–original draft, Writing–review & editing. Kangcheung Chan: Formal analysis, Writing–review & editing. Shunzhi Qiao: Investigation, Measurement. Kai Zhang: Investigation, Software, Measurement. Taiman Yue: Formal analysis. Zhongning Guo: Conceptualization, Methodology, Supervision, Resources. Jiangwen Liu: Supervision, Resources, Writing–review & editing.

Declaration of competing interest

The authors declare that they have no known competing financial interests or personal relationships that could have appeared to influence the work reported in this paper.

Acknowledgments

The work described in this study was supported by the National Natural Science Foundation of China [Grant Nos. 52075104 and 52175387].

References

[1] C. Hnatovsky, RS. Taylor, E. Simova, PP. Rajeev, DM. Rayner, VR. Bhardwaj, PB. Corkum, Fabrication of microchannels in glass using focused femtosecond laser radiation and selective chemical etching. Appl Phys A-Mater 2006; 84: 47-61.

[2] Yang F, Han, GW, Yang J, Zhang M, Ning J, Yang FH, Si CW. Research on Wafer-Level MEMS packaging with through-glass vias. Micromachines 2019; 10:1-5.

[3] Sukumaran V, Kumar G, Ramachandran K, Suzuki Y, Demir K, Sato Y, Seki T, Sundaram V, Tummala RR. Design, fabrication, and characterization of ultrathin 3-D glass interposers with through-package-vias at same pitch as TSVs in silicon. IEEE T Comp Pack Man 2014; 4: 786-795.

[4] Pandey H, Singh T, Dixit P. Formation of high aspect ratio through-glass vias by the combination of Ultrasonic micromachining and copper electroplating. J Manuf Process 2022; 82:569-584.

[5] Kumar N, Mandal N, Das AK. Micro-machining through electrochemical discharge processes: a review. Mater Manuf Process 2020; 35: 1-42.

549 [6] Kurafugi H, Suda H. Electrical discharge drilling of glass. Ann CIRP 1968;16: 415-419.
550 [7] Singh T, Dvivedi A. Developments in electrochemical discharge machining: A review on
551 electrochemical discharge machining, process variants and their hybrid methods. Int J Mach Tool
552 Manuf 2016;105: 1-13.
553 [8] Kannojia HK, Arab J, Pegu BJ, Dixit P. Fabrication and Characterization of Through-Glass Vias by
554 the ECDM Process. J Electrochem Soc 2019;166: 531-538.
555 [9] Arab J, Mishra DK, Kannojia H.K, Adhale P, Dixit P. Fabrication of multiple through-holes in non-
556 conductive materials by Electrochemical Discharge Machining for RF MEMS Packaging. J Mater
557 Process Technol 2019;271: 542-553.
558 [10] Arab J, Kannojia HK, Dixit P. Effect of tool electrode roughness on the geometric characteristics
559 of through-holes formed by ECDM. Precis Eng 2020; 60: 437-447.
560 [11] Zheng, Zhi-Ping, Su, Hsin-Chuan, Huang, Fuang-Yuan, Yan, Biing-Hwa. The tool geometrical
561 shape and pulse-off time of pulse voltage effects in a Pyrex glass electrochemical discharge
562 microdrilling process. J Micromech Microeng. 2007;17: 265–272.
563 [12] Chen, Jia-Chang, Lin, You-An, Kuo, Chia-Lung, Ho, Chao-Ching, YAU, Wing-Hing. An
564 Improvement in the Quality of Holes Drilled in Quartz Glass by Electrochemical Discharge
565 Machining. Smart Science. 2019;7: 169–174.
566 [13] Appalanaidu, Botcha, Dvivedi, Akshay. On the use of sacrificial layer in ECDM process for form
567 accuracy. J Manuf Process. 2022;79:219-232.
568 [14] Huang L, Cao Y, Jia F, Lei Y. Study on the stability of gas film in electrochemical discharge
569 machining of ultra-white glass micro array holes. Microsyst Technol 2020; 26:947-955.
570 [15] Wuthrich, R, Hof, LA. The gas film in spark assisted chemical engraving (SACE)—A key element

for micro-machining applications. Int J Mach Tool Manuf 2006;46: 828-835.

[16] Tang, WD, Kang, XM, Zhao, WS. Enhancement of electrochemical discharge machining accuracy and surface integrity using side-insulated tool electrode with diamond coating. J Micromech Microeng. 2017;27: 065013.

[17] Yang CK, Wu KL, Hung JC, Lee SM, Lin JC. Enhancement of ECDM efficiency and accuracy by spherical tool electrod. Int J Mach Tool Manuf 2011; 51: 528-535.

[18] Singh T, Dvivedi A, Shanu A, Dixit P. Experimental investigations of energy channelization behavior in ultrasonic assisted electrochemical discharge machining. J Mater Process Technol 2021; 293:1-14.

[19] Elhami S, Razfar MR. Study of the current signal and material removal during ultrasonic-assisted electrochemical discharge machining. Int J Adv Manuf Technol 2019; 92: 1591-1599.

[20] Jiang BY, Lan SH, Wilt K, Ni J. Modeling and experimental investigation of gas film in micro-electrochemical discharge machining process. Int J Mach Tool Manuf 2015; 90: 8-15.

[21] Laio YS, Wu LC, Peng WY. A study to improve drilling quality of electrochemical discharge machining (ECDM) process. Procedia CIRP 2013; 6: 609-614.

[22] Sabahi N, Razfar MR. Investigating the effect of mixed alkaline electrolyte (NaOH + KOH) on the improvement of machining efficiency in 2D electrochemical discharge machining (ECDM). Int J Adv Manuf Technol 2018; 95: 643-657.

[23] Sabahi N, Razfar MR, Hajian M. Experimental investigation of surfactant-mixed electrolyte into electrochemical discharge machining (ECDM) process. J Mater Process Technol 2017; 250: 190-202.

[24] Kunieda M, Kitamura T. Observation of Difference of EDM Gap Phenomena in Water and Oil

Using Transparent Electrode. Procedia CIRP 2018; 68: 342-346.

[25] Dörner P, Schröder W, Klaas M. Experimental quantification of oscillating flow in finite-length straight elastic vessels for Newtonian and non-Newtonian fluids. Eur J Mech B-Fluid 2021; 85:180-195.

[26] Zou ZX, Guo ZN, Zhang K, Xiao YJ, Yue T.M, Liu JW. Electrochemical discharge machining of microchannels in glass using a non-Newtonian fluid electrolyte. J Mater Process Technol 2022; 305: 117594.

[27] Lu YB, Tang GH, Tao W.Q. Experimental study of microchannel flow for non-Newtonian fluid in the presence of salt. Exp Therm Fluid Sci 2016;74: 91-98.

[28] Singh T, Dvivedi A. On performance evaluation of textured tools during micro channeling with ECDM. J. Manuf. Process 2018; 32: 699-713.

[29] Kolhekar KR, Sundaram M. Study of gas film characterization and its effect in electrochemical discharge machining. Precis Eng 2018; 53: 203-211.

[30] Arab J, Dixit P. Influence of tool electrode feed rate in the electrochemical discharge drilling of a glass substrate. Mater Manuf Process 2020; 35: 1749-1760.

[31] Singh, Tarlochan, Dvivedi, Akshay. Fabrication of micro holes in Yttria-stabilized zirconia (Y-SZ) by hybrid process of electrochemical discharge machining (ECDM). Ceram, Int 2021;47: 23677-23681.

[32] Elhami S, Razfar MR. Analytical and experimental study on the integration of ultrasonically vibrated tool into the micro electro-chemical discharge drilling. Precis Eng 2016; 47: 424-433.

[33] Marshall, JS. Viscous damping force during head-on collision of two spherical particles. Physics of Fluids 2011; 23:5382-143.

615 [34] Tang GH, Li XF, He YL, Tao W.Q. Electroosmotic flow of non-Newtonian fluid in microchannels.

616 J Non-Newton Fluid 2009; 157:133-137.